A Control System for Bionic Shoes

Xunjie Zhang

CMU-RI-TR-17-39
July 2017

School of Computer Science
Carnegie Mellon University
Pittsburgh, PA 15213

Thesis Committee:
Randy Sargent, Chair
Chris Atkeson
Jennifer Cross

Submitted in partial fulfillment of the requirements for the degree of Master of Science in Robotics.

Abstract

The fact that many residences and businesses lay beyond an easy walking distance to a public transit stop is known as the ”last mile problem”, and is a barrier to better utilization of a rapid transit network. Alternative modes of transportation including bicycles, Segway, scooters, and motorcycles all promise to fill this gap, but none of them have really solved this problem due to their risky nature or difficulty to use. In this thesis, we present the development of a control system of a pair of bionic shoes that enable average pedestrians to walk twice as fast. The experience is similar to walking on the moving walkway - shoes adapt to your gait thereby making them a natural extension of your legs. In this thesis, we described an interdisciplinary approach through customer development, design thinking and addressing key bipedal walking challenges.

Acknowledgments

I would like to thank my advisor Randy Sargent for his advice, constant support and encouragement. I would like to thank Professor Chris Atkeson and Jennifer Cross for their inspiration and feedback. I would like to thank my family for their financial and mental support. I would also like to thank Professor Dave Mawhinney from Swartz Center for Entrepreneurship for his business advice. I would thank Anand Kapdia from Electrical and Computer Engineering Department for helping me on firmware and circuits design. I would like to thank Brian Chan, Zulay Olivo from Tepper school of business and Yubing Zhang from Integrated Innovation Institute on helping to conduct customer discovery and user study. At last, I would thank all of my colleagues at CREATE lab for their support and collaboration.

Contents

List of Figures

List of Tables

Chapter 1: Introduction

Approximately 17.5 million daily commuters walk or take public transit in the US, according to McKenzie [17]. Unfortunately commuting around metro areas is frustrating, slow and expensive. In spite of public transportation being the most time-efficient and affordable choice for most commuters, getting to and from the nearest transit stop is still a major barrier for mass commuters to leverage mass transit. The average new yorkers spend over 48 minutes walking as part of their commute everyday, which is equivalent to 131 hours annually, as show in fig. 1.1. This issue is known as the first/last mile.

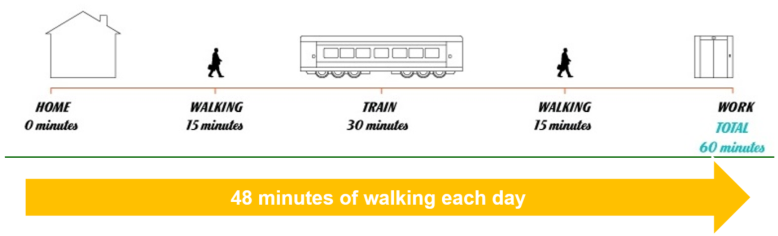

Figure 1.1: First/Last mile problem

One natural solution to the first/last problem is to live closer by the transit stop. However, this solution introduces additional cost on commuters' rental cost. For instance, commuters in New York city pays \$56 per month more for every minute closer by subway, based on Bialik [3].

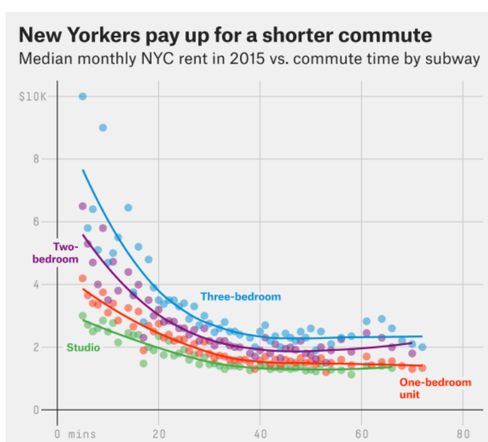

Figure 1.2: Commuting time vs Rental cost in New York

Alternative modes of transportation including bicycles, Segways, scooters, and motorcycles all have the potential to help fill this gap, but none of them have really solved the problem well enough for the average commuters. Bikes are legally required to share roads with vehicles, putting riders in dangerous situation. They are also too large to bring onto most mass transit or cars. Segways do not fit well on sidewalks and also are too large to bring on mass transit or cars. Skateboards and roller skates are unsafe to be on street, and cannot be used on high-density sidewalks. None of the above can go onto stairs and all have a very steep learning curve.

Our solution is a pair of motorized wheeled shoes, called Nimbus that increase pedestrians walking speed without extra effort, saving up to half of the commuting time. Nimbus are so convenient that you can wear them throughout the entire commute - going on/off stairs and public transports without ever taking them off. The original prototype (see fig. 1.3) that consists of a pair of wheeled shoe-platforms, which is driven by a single brushless DC motor via timing belts.

Figure 1.3: The original prototype

Chapter 2: Customer development

A lot of developers often fall into the trap of starting with a product idea that they think people want and spend months or even years perfecting the product without understanding customers' needs, which could ultimately lead to a product that no one cares. Therefore, in order to build a product that people want, we focus on building a product through validated learning, a concept first described in Ries [23]. The learning process includes validating the first/last mile problem through customer discovery, determining and prioritizing the core features to develop through design thinking, and learning from target customers through rapidly shipping engineering iterations on a regular interval.

"Should the motorized shoes ever be built?" - This is the most fundamental question that we ask ourselves. Moreover, who are our target customers and what is their pain point[1]? With those questions in mind, We worked with MBA students from Tepper School of Business to carry out surveys on 97 potential users with various commute modes(driving, biking, walking and public transit), ages between 18 and 35, and annual income ranges between $50K and $150K. We ask them about their preferred commute method, distance and cost of commute, frustration points, which has allowed us to propose and validate a set of hypothesis around customers and their pain points.

2.1 Hypotheses

We came up with three fundamental hypotheses around customers, problem and solution.

- **Customers**: Cyclists, skateboarder, segway riders, and roller-skate users who commute on a daily basis (for work and recreation).
- **Problem**: Commuting is time consuming, dangerous, and expensive. The current alternatives are difficult to master, not intuitive for first time users, or too bulky to store.
- **Solution**: Nimbus are incredibly easy to use and enable you to walk twice as fast, arrive at your destination in less time while costing a fraction of your commute.

2.2 Customer empathy map

We validated the above hypotheses by conducting structured interviews among a group of 97 commuters living in various US cities including Boston, Pittsburgh, New York and San Fran-

[1] A conceived or real problem that entrepreneurs aim to solve

cisco. We then created a customer empathy map[2] to gain an more empathic understanding in their pain points and visualize what an ideal customer is like. The interview among our focus group, consists of three sections - problem, current situation and proposed solution. Once the interview was done, we created customer empathy map from the data to gain a deeper insight into our customers and build out a user story. This is done through exploring the vicarious experience and intellectual identification with the feelings, thoughts and attitudes, see fig. 2.1.

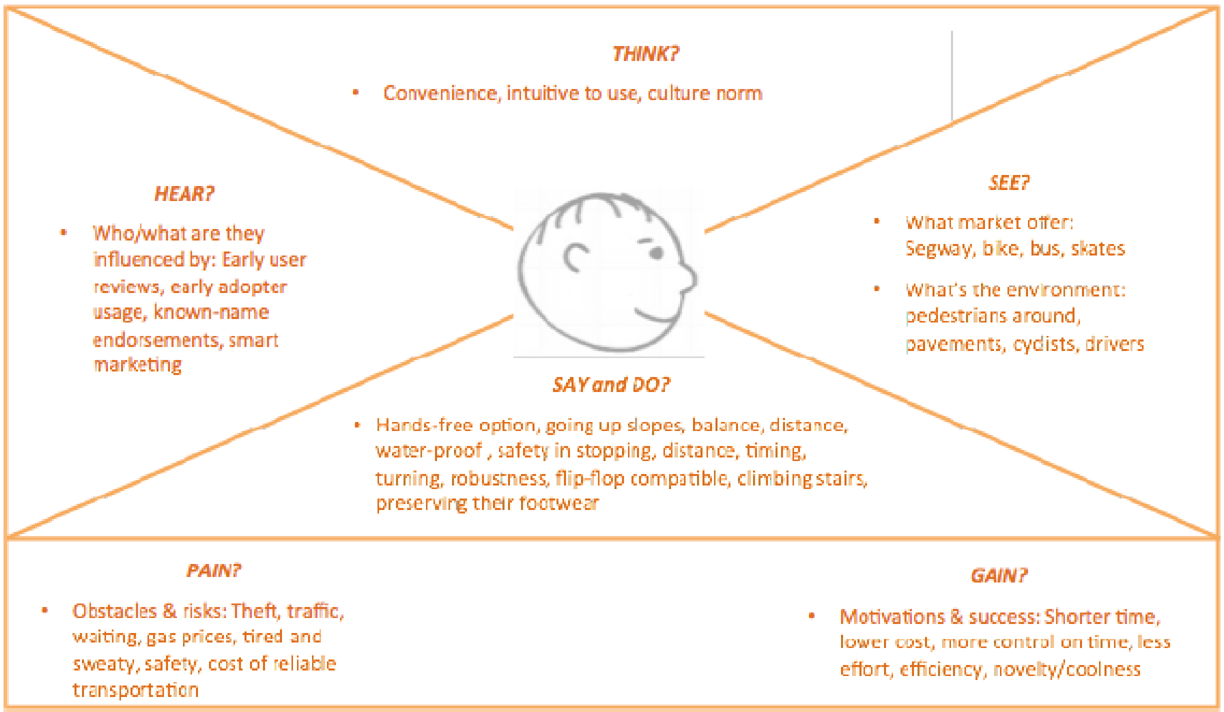

Figure 2.1: Nimbus customer empathy map

- **Customers**: We found our validation was different from our hypothesis. Our target customer segments are now people who walk regularly for their commute, or people who would use the shoes for fun and recreation. Those people tend to live in a metro area where taking public transport is significantly more efficient and cost-effective than driving. Furthermore, we exclude those "die-hard" users who have significant emotion and identity attachment to their bikes, roller-skates, or skateboards.
- **Problem**: The hypothesis was validated here as people do feel the pains of current commuting options and other alternatives. The lack of reliable and affordable transportation options is a critical pain point.
- **Solution**: The hypothesis was partially validated: a) The product is particularly popular for 2-3 mile commutes. b) The product cuts out the uncertainty and waiting time of commuting with portability and theft-proof over bikes. c) People who are tech-savvy demonstrate

[2]Empathy maps are a gathering of information that depicts your ideal customer.

tremendous interests and curiosity towards the product and are willing to invest in a personal robotic technology. d) Many compared it to smart phone and bikes for a price point. e) Those ”die-hard” users were unwilling to see the value proposition over their bikes or skateboards as the augmented walking reduces their exercise and the sense of achievement over mastering a challenging activity. f) An affordable price is also an important factor on customers’ purchasing decision.

2.3 User persona

Based on the survey results, we developed a persona to evaluate our solution. Kevin Chan, a young software engineer and a city commuters working in the downtown Boston. He starts his commute by walking for 20 min to the nearest subway stop, then spends another 10 min on the subway and completes his commute with another 20 min walk to his office.

2.3.1 A day in the life - before

- **Desired outcome** Kevin wants to find an alternative to reduce the walking part of his commute. As a software developer, he rarely get any exercises during the day. But he values staying active and healthy, enjoys being outdoor when the weather is good so that he can unplug. At the same time, he also want to minimize commuting logistics such as walking to public transit, need for showering, and changing shoes.
- **Attempted approach**: He has looked into several alternatives: a) Driving and parking is time-consuming and expensive, b) Biking is possible but vulnerable to theft which is equal to high cost. Biking is also too sweaty and is only allowed on subways during off-peak hours. c) He did a lot of skating when he was a teenager but unfortunately skating involves too much physical exertion and is too risky on the busy road.
- **Consequence**: He has not committed into any of the alternatives and is not happy with the current situation.

2.3.2 A day in the life - after

- **New approach**: By walking in the motorized shoes to the bus stop, Kevin is able to speed up his walking without extra effort.
- **Reward**: He now can commute reliably for only 30 minute in total. Not only he can save recurring bus/subway fee during good weather, but also choose to start commuting without worrying about bus schedules and traffic. He loves being outside when the weather is good and does not worry about theft as the shoes can be easily stored in a backpack or under an office desk.

2.4 Conclusion

Through customer discovery, we have identified the target customers of Nimbus shoes, validated the problem space of first last mile and learned the unique scenarios to apply Nimbus technology.

Chapter 3: User centered design

Following the completion of the customer discovery and creation of persona, we next create a set of product requirements that can be translated into a set of engineering specifications. We conducted a series of co-design activities with the perspective users over three months period and analyzed their interaction with the original prototype, see fig. 1.3.

A total of 9 interview subjects were chosen from Tepper School of Business as all of them have worked in large metro areas for at least 6 months. Their demographics include:

- 7 males and 2 females
- Ages from 25 to 30
- Commuting distance from 1 to 10 miles
- Transport modes from driving, walking and bus taking
- Income from $75k to $150k

The sample is slightly biased, in that a) all subjects are studying business and are in the same school; b) although subjects have lived and commuted in different metropolitan areas in the US, they all only commute to the business school at the time of interview; c) all the subjects have lived in the US all their life.

3.1 Key activities

We have conducted design interviews on two groups of subjects and each interview consists of three activities - experience description, expectation description and usability tests. Both interviews take place in the first three months of the project.

3.1.1 Experience description

In this exercise, each user is asked to describe their commute experience from their home to the workplace in great details, which include their positive and negative emotions, transportation mode and any particular events or objects of interests.

The following table summarizes users' commute experience on different modes of transportation. The number in bracket shows the number of interviews responded. Note one subject can respond with multiple choices. In addition to the cost of transportation, predictability is ranked more important than cost of time. This is probably because a predictable and reliable commute mode allows for better planning even sometimes such mode of commute can take a little longer than others.

Mode of Transportation	Pros	Cons
Driving (3)	Comfortable	Lack of exercise, parking is expensive and time-consuming
Walking (9)	Exercise, joyful experience, save money, total control	Time-consuming
Taking bus (5)	Cheaper than driving	Unreliable, possibility of missing bus time, crowded buses and cannot deal with emergency

Table 3.1: Commute experience based on modes of transportation

3.1.2 Expectation description

After the experience description, users then came up with their own ideas on how this experience can be improved and what are the most important criteria to their experience. In order to not limit the possible solutions, we intentionally offered out-of-box ideas to users in our prompt words (see fig. 3.1). The goal was not only to figure out the key elements that influence commute experience but also to gauge how readily the consumers accept new mobility technology.

Wheel	Shoes	Comfortable	Spacecraft
Blanket	Skiing shoes	Beautiful	Fancy
Magic	Car	Comfortable	Reliable
Fast	Cart	Easy-to-wear	Stable
Exiciting	Colorful	Easy-to-walk	Smart
Carzy	Adventure	Belt	Safe
On-time	Efficient	Relax	Control

Figure 3.1: Prompt words to describe potential solutions

We learned several key criteria that users consider when adopting a new mode of commute:

- Safety: every participant highlighted safety as their top priority. Not only does the product have to be safe and reliable but also easy to control and steer on sidewalks.
- Reliability and predictability: all users expect the technology to work without faults for a long time due to the mission critical nature of the commute.

- Convenience: the technology should be plug and play as well as easy to carry around.
- Familiarity of the user interface: most of the users preferred a powered shoes to augment their walking instead of those more blue-sky designs such as teleporting and flying cars. Although people are always excited about new technologies, they also want to have a sense of familiarity in adopting a new mode of transportation. Not surprisingly, the ability to augment our walking motion was seen by interviewed users as the easiest to adopt.

3.1.3 Usability test

Next, we sought to understand the overall experience of using the original prototype (see fig. 1.3) through a range of actions:

- Putting on the shoes
- Getting used to balancing on the elevated platform
- Walking on the leveling ground
- Accelerating and decelerating on the leveling ground
- Turning gently and sharply
- Walking on carpet, hard floor and concrete.

The only instruction given prior to this test was how to use a hand-held joystick to control the speed. The further joystick is pushed away from the neutral position, the faster shoes moves. We analyzed users' direct feedback and the recorded videos to establish a more insightful understanding of their behavior and the root causes. The questions we considered were:

- How does the user figure out the use of strap mechanism and tighten up the buckle?
- What preparation does the user make before they start to roll?
- How does the user react to the first acceleration?
- How does the user respond to low / high speed as well as acceleration?
- How does the user handle turning?
- How natural and stable does the user walk? How do they feel?
- How easy is it for the user to take off the shoes?

So we found four major issues observed during the usability test. The first issue was the speed controller. There is a lack of intuitive relationship between the joystick movement and the acceleration of the motorized shoes as the allowable joystick movement was so short and any small movement translates into a drastic acceleration. After the user adjusts to the acceleration and deceleration while walking straight, they still often forget to reduce the speed when making the turns. The joystick control requires significant amount of attention, which causes stress when using the shoes.

The second issue was that the users are unwilling to perform walking in the motorized shoes, instead, they skate. The weight, platform height, size of the shoes and rigidity of the platform significantly hinder users' ability to walk and draw a closer analogy to skates.

The third issue was the perception of safety. The appearance of the motorized shoes was so alien from everyday walking shoes that all the users thought they were more risky to use than they actually are. There also seem to be a lack of clear instruction to get through the learning curve as quickly as possible. Many users fail to start walking with the shoes held stationary before accelerating the shoes, causing them to lose their balance. This negatively impacts on users' initial confidence and experience in adopting to the shoes.

The last issue was about perceiving the device as shoe attachment over actual shoe. It was clear that users see the device more as a mode of commuting rather than a permanent wearables that you have them on all the time. Not only are shoes more personal and cultural but people wear shoes to identify themselves. Positioning our device as shoes takes away those benefits.

3.2 System requirements

Through user centered design, we have seen an opportunity to design beyond motorized shoes. We decided to create a pair of bionic shoes which offer more organic, intuitive and smooth experience to the users. This will requires a more ergonomic and flexible mechanical design, with an intelligent controller that matches the movement of the device with human motions. Here are the functional and non-functional requirements.

Operational Requirement

- The device shall enable the user to walk twice as fast in the most intuitive and natural fashion.

Functional Requirements

- The device shall move at a wide range of speeds. (Rationale: the bionic shoes have to be sufficiently slow for users to adapt initially and fast enough to save up meaningful amount of commute time)
- The device shall provide a set of mechanical structure that allow users to walk naturally. (Rationale: to satisfy safety and convenience expectation)
- The device shall allow users to walk up and down the stairs without taking it off. (Rationa: to satisfy convenience expectation)
- The device shall provide an intuitive means of control that minimize the learning curve. (Ration: to satisfy the expectation of familiar user interface)

Non-functional Requirements

- Each shoe should weigh no more than 1kg in total.
- The device should be able to fit into an average backpack.

Chapter 4:   Physical Hardware

4.1   Related products

Chavand [6] developed a walkings device that consists of an upper plate mounted on a chassis resting on a set of four wheels in contact with the ground. The lateral articulation to allow natural movements of the heels with respect to the toes during normal walking. There is also a interconnected spring mechanism at both the front and rear such that the front extends and the rear compresses during the heel-strike and vice versa during the push-off phase. A set of larger wheels on each side of the shoe attempt to provide lateral stability. The pressure sensor under the front plate is directly proportional to the acceleration which is only activated when the heel is lift off. A small dc motor coupled with a flywheel and a gearbox is used to maintain a set speed. There are a few issues with this design: a) large wheels on the side of mid-foot area do not provide sufficient stability during push off stage as the most of ground reaction force is concentrated around ball area; b) accelerating the shoe during the single stance phase means a much smaller base Of support (BOS) causes walking instability; c) the height of the shoes further exacerbate walking instability for walking; d) the flywheel has little use in speed control but only adds extra weight.

Figure 4.1: Rollkers

Acton Rocket Skates developed by Treadway et al. [26] are a pair of motorized skates that use tilt signal to control the motion. Only the primary skate is installed with a tilting sensor while the second skate takes instructions from the primary one. To use the skates, user has to place the second skate in front of the primary one and lean back slightly to trigger the tilting sensor. This control method is fundamentally flawed in the way that center of mass (COM) frequently moves ahead of base of support (BOS) during bipedal walking motion.

Figure 4.2: Acton Rocket Skates

4.2 Design iteration

Our design and manufacture partner helped us to design and construct four major iterations(from MK1 to MK3), as shown in Figure 4.3 to achieve an optimal trade-off among flexibility, stability, ground clearance and weight. As the focus of this thesis is on the development of the control system, the physical hardware is shown here for context but not described in detail.

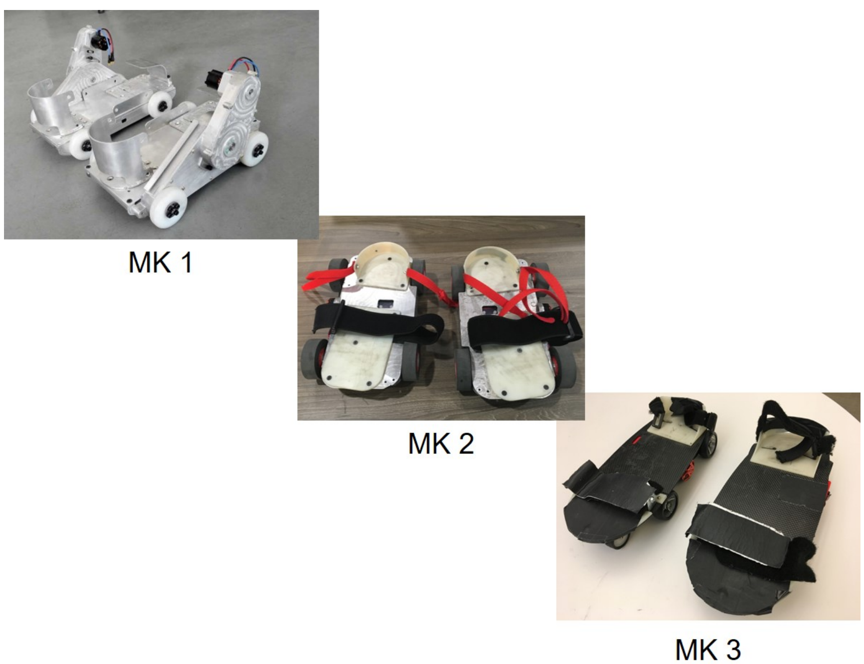

Figure 4.3: Prototype Iterations

Table 4.1 explains the major improvement points and drawbacks of each prototype iteration.

Iterations	Enhancement	Issues
MK 1	Improve stability by lowering the platform height and increasing its width	Heavy weight due to large metal components and overall bulkiness
MK 2	Preserve stability while reducing the weight	Wide and rigid platform
MK 3	Introduce a flexible structure	Lack of transmission power

Table 4.1: Design rationale for each iteration

Chapter 5: Gait detection

5.1 Bipedal walking challenge

Understanding the gait dynamics is critical to sizing power system and controller design. A gait cycle consists of two phases: stance (60% of gait cycle) and swing phase (40% of gait cycle). Stance phase starts with the heel strike - this is the moment both vertical and horizontal ground reaction forces (GRF) will start rising to their peak values. The vertical peak GRF gives the max impact load that the chassis has to withstand without significant distortion, while the negative horizontal GRF must be less than the max force that the power system can output such that users do not slip forward. In the midstance phase, the body begins to move from force absorption at impact to force propulsion forward, according to Shultz et al. [24]. Push-off phase occurs before transitioning into swing phase, resulting in another peak of vertical GRF and a positive horizontal GRF, both of which are the design points of power system as well.

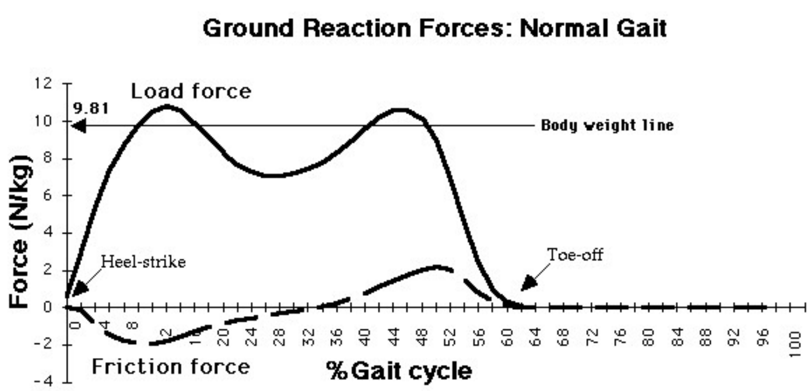

Figure 5.1: Gait Cycle and its corresponding GRFs[2](solid line is vertical GRF, dotted line is horizontal GRF)

There are three main challenges associated with walking balance, as suggested in Winter [28]. The first challenge is to restablize the body center of gravity (COG) when it is far beyond BOS. In order to accelerate our body in a forward direction, the body has to accelerate the COG ahead of BOS, while during the heel strike phase, COG must return within the base of support. As seen in fig. 5.2, since COG is so far off from the support base during acceleration, both hip

[2]Image Courtesy of Cuccurullo [8]

and ankle strategy is no longer able to avert a fall, only foot placement of the swing foot will allow restablization. But the support base is not firm as one foot is absorbing the impact from heel strike and the other is pushing off.

The second challenge is that two thirds of our body weight - head, arms and trunk(HAT) is located at two-thirds of body height above the ground. This is dynamically similar to an inverted pendulum which is inherently unstable considering the forward momentum of the truck and head seen in fig. 5.2

Finally, the large inertial load of HAT has to be maintained erect within $\pm 1.5°$ with significantly attenuated head accelerations. Controlling such a system for steady-state walking is near impossible so only dynamic stability can be achieved.

To offer the most natural interaction between the shoes and user, the controller must be able to determine the user gait (heel strike, midstance and push-off etc) in real-time so that it can accelerate or decelerate appropriately without introducing excessive disturbance to the walking motion. Furthermore the controller will be able to determine between walking and other motions such that the bionic shoes will only start and stop as per user's intention.

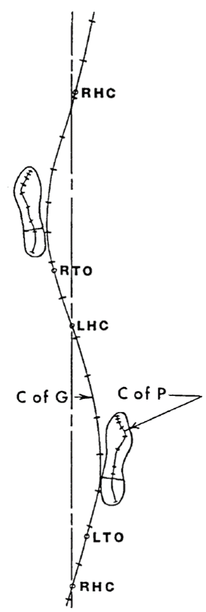

Figure 5.2: Total body CoM and CoP under support feet during level walking[3]

Two approaches were implemented and evaluated: virtual modeling predication and machine learning classification. For the purpose of simulation, we applied virtual model control (VMC) proposed by Pratt et al. [22] for bipedal walking simulation. If the virtual model can produce representative GRFs, we can create a inverse virtual model to interpret subjects current gait. Furthermore, we collected true GRFs from multiple human subjects performing normal walking on the prototypes to train a classification model via Singular Vector Machines (SVMs).

[3]Image Courtesy of Winter [28]

5.2 Gait detection - VMC

Virtual Spring-damper components are attached to the robot in three axes (Z,X,theta). Each component is responsible for stabilization task in height, pitch or forward velocity using PD control. The term virtual means the calculated torques create the same effects as if the physical components are connected with the real robot, as shown in fig. 5.3. The component forces are calculated and converted to joint torques by Jacobian relation. Virtual Spring-damper components are attached to the robot in three axes (Z,X,theta), controling the height, pitch and forward velocity as indicated by Hu et al. [11].

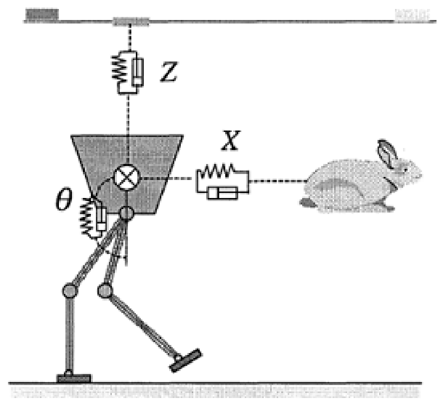

Figure 5.3: VMC Implementation [4]

5.2.1 Model

The model is separated into three parts: mechanics, controllers and state machine. The walking mechanics has a trunk with two legs located at the same hip joint location. The ankle joint was connected to the planar ground interaction model since we assume the foot as a point (no feet model used). Parameters like position, angle, velocity and joint torques are transferred between walking mechanics and controllers. The state machine decides which controller to enable and correctly apply torques to actuate joints. There are two single support states and one double support state in this model. Double support is enabled when both legs are contacted with the ground. Single support is enabled when one stance leg is on ground and another leg is in swinging.

Height and pitch control are applied in all states. Velocity control is implemented during the double support. Swing leg control is based on the mirror law, which means the angle of swing leg should always duplicate the angle of stance leg. The angle is measured between the line connecting ankle to hip and the vertical line. During the entire swing phase the knee is bent to not drag on the ground. The knee joint's torque is set to zero when body's position becomes further than a preset distance from the support foot instead of when reach a nominal stride length wrote in the paper.

[4]Image Courtesy of Hu et al. [11]

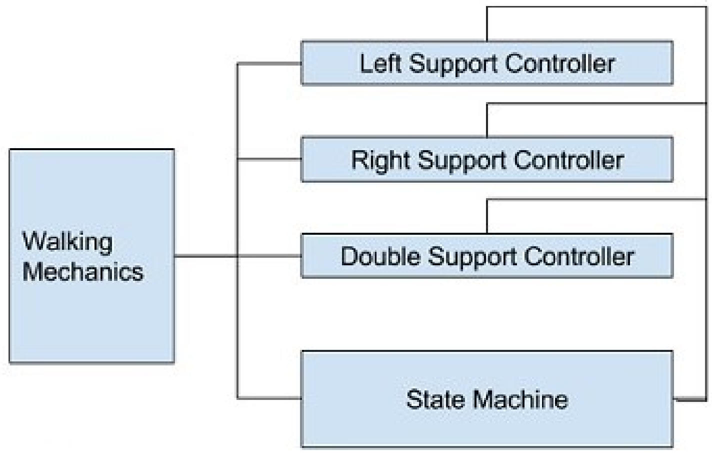

Figure 5.4: State machine used in gait simulation

5.2.2 Results

We achieved a VMC bipedal model that is able to walk for 10 steps before it goes unstable. In the simulation, the bipedal model starts from a single support pose with a short pulse of initial horizontal force applied on the body. With a large knee bending, the model is dissimilar to the normal walking gait. The body pitch angle shown in fig. 5.5, although oscillates continuously, tracks the desired upright angle (0°). As the model moves forward, the stride length increases to a peak value and then decreases after a few steps.This can also be viewed in terms of body horizontal velocity, as show in fig. 5.6, which reaches the peak (over 1m/s) at around 8th step. The height regulation as depicted in fig. 5.7 shows an rising trajectory gradually deviates away from the desired height by 10%. The max vertical GRF increases after each stride as shown in fig. 5.8 reveals an unexpected high impact force at the point of each foot striking on the ground.

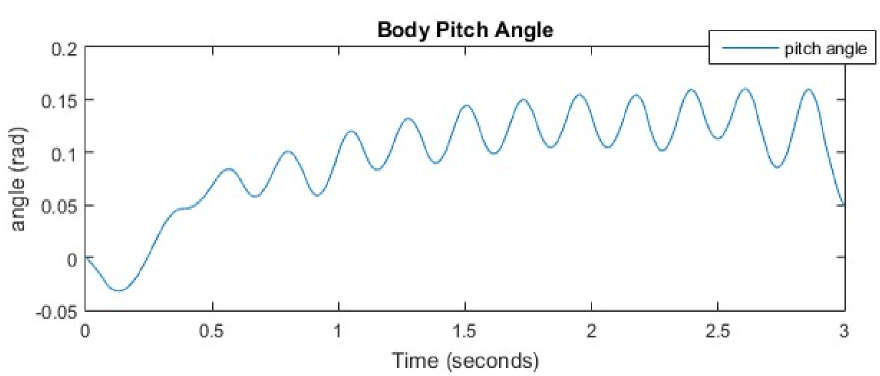

Figure 5.5: Simulation results - body pitch angle

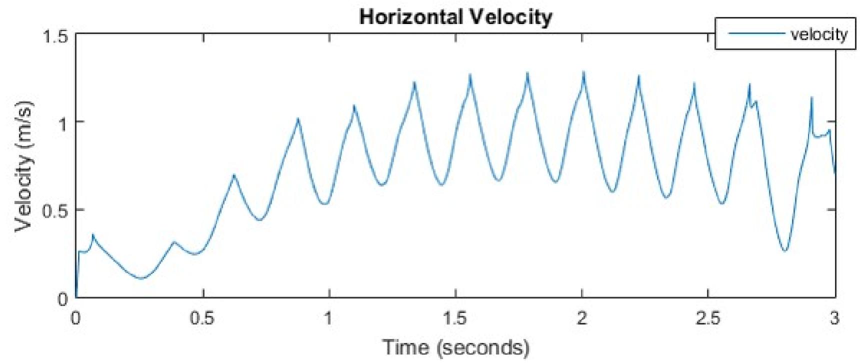

Figure 5.6: Simulation results - horizontal velocity

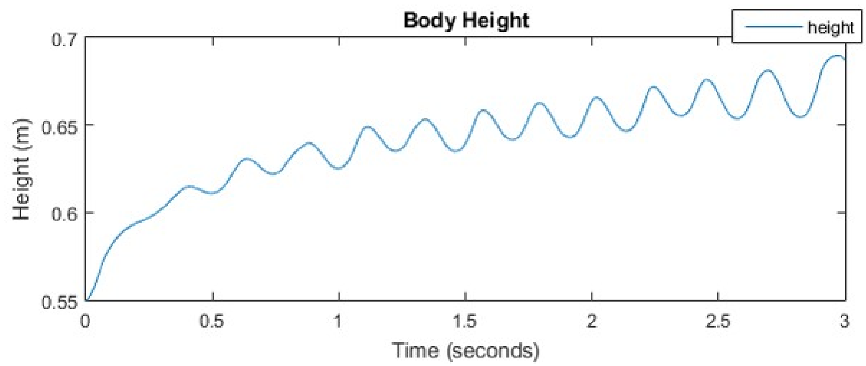

Figure 5.7: Simulation results - body height

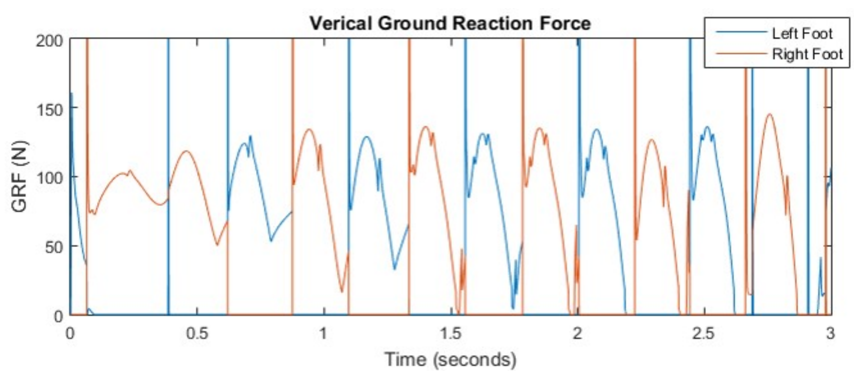

Figure 5.8: Simulation results - vertical ground reaction force

5.2.3 Conclusion

This study has shown that VMC bipedal model is not suitable for generating representative GRFs reliably. The model failed to demonstrate human-like walking dynamics. Comparing with the experimentally obtained GRFs from Browning and Kram [4], we failed to replicate double-hump pattern of a typical GRF curves. This could have be caused by the incorrect model parameters and gains. However the difficulties of tuning a set of parameters renders the model generated GRFs approach is less likely to generalize. The high impact force during the initial landing is also unavoidable due to the rigid segment components. In the future, other models such as adaptive VMC with flexible parameters and muscle reflex model could be attempted to avoid high impact loss caused by rigid segments. Though the model based approach work for a specific set of configurations, it is not clear if it will be able to model all types of gaits. So we decided to not pursue with the model-based method further.

5.3 Gait detection - SVM

5.3.1 Related work

There are extensive work on gait analysis from clinical literature. Temporal and spatial gait parameters are obtained and analyzed using machine learning techniques. Zhang et al. [30] use Bayesian classifier to identify healthy walking gait from those with spastic diplegia. They used stride length and cadence data collected from children walking experiments. Hundza et al. [12] distinguished people with Parkinson's disease using gait cycle data measured by Inertia Measurement Unit (IMU), and achieved 100% accuracy on 13 test subjects. Also, gait cycle detection is done using manually defined heuristic rules. Lee and Grimson [15] use SVM on human walking video data to classify individuals.

In robotics community, GRF serves as a key indicator of bipedal walking stability. Vukobratović and Borovac [27] proposed a walking balance criterion based on GRF distribution. One popular application in bipedal walking is done by Kajita et al. [13]. In human experiments, Popovic et al. [21], and Cavanagh and Lafortune [5] also shows the correspondence between ground reaction force and human walking/running state.

To use GRF in gait analysis, Muniz and Nadal [19] applied Principle Component Analysis (PCA) on complete stride GRF data to identify unhealthy gaits. Each sample was the GRF profile of a 10s continuous walking data. Moustakidis et al. [18] pre-processed the GRF data with wavelet packet (WP) for feature selection, then trained a Support Vector Machine (SVM) to do subject recognition. Muniz et al. [20] evaluate the effectiveness of Parkinson disease treatment using typical classifiers including probabilistic neural network, SVM and logistic regression. Alaqtash et al. [1] used artificial neural network and nearest neighbor classifier on 6-axis GRF data, and achieve 95% accuracy in pathological gait pattern detection.

There are fewer works on real-time gait prediction/classification. Cutler and Davis [9] used vision data and computer vision technique to detect human walking gait on a treadmill. Skelly and Chizeck [25] used four in-sole force sensitive sensors (FSR) in each shoe with a Fuzzy-logic classification rule, achieved 86% accuracy on heel-strike/push-off prediction.

5.3.2 Data collection

In order to collect GRFs during walking, we attached force sensitive sensors (FSR) to the sole of each bionic shoe. Two in the front for measuring push-off and one at rear for measuring heel-strike. This is illustrated in fig. 5.9. The FSRs are slightly higher than the sole plane, so as to capture most of the normal contact force. During data collection, the user use a remote controller to signal his/her intention of walking, which is used as the data label.

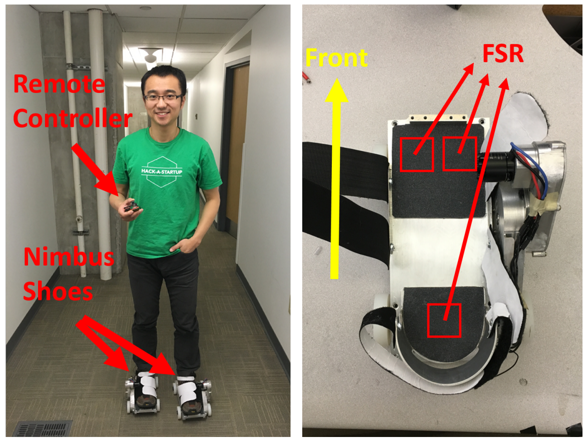

Figure 5.9: The data collection hardware setting

5.3.3 Algorithm

A Support Vector Machine is a discriminative classifier with linear decision boundary in the hyperplane. Since the training set is unlikely to be linear, we used th Radius Bias Filter (RBF) kernel to project the training data into hyperplane where linear decision boundary can be drawn.

We took a Fast Fourier Transformation (FFT) on each sensor dataset to obtain the dominant frequency and the magnitude at the dominant frequency. To express the temporal interdependency between front and back sensors, we subtracted the front sensors from back sensor readings then take the magnitude and the phase shift between the peak and trough of each subtractions.

We train the classifier based on both the fast and normal walking gait data, and test the classifier on varying-speed gait data. F-measure, a measure of testing accuracy, was used to assess the classifiers performance which will be discussed in the Result section.

We used Adaboost (or Ensemble) method has been used on the SVM in attempt to achieve an enhanced test performance. The idea is that instead of using a single strong SVM classifier, multiple weak SVM classifiers which are good at different parts of the input space will be trained. We start with a uniformly distributed weights for each training example. Then for each iteration t, we increase the probabilistic weights of each misclassified training example so that the next learned classifier can specifically target those points. At the same time, we record the strength for each classifier α_t. Finally, each weak classifier with their corresponding strength is added together to create a final classifier

$$H(X) = sign(\sum \alpha_t h_t(X))$$

5.3.4 Results

The result of a single SVM classifier is shown in fig. 5.10, where the first and second subplots show all sensory readings on both shoes, while the last subplot shows the correctly predicted labels (area in green) and incorrectly predicted labels (area in red). This single baseline classifier has achieved 91.32% accuracy on the test set with 93.43% precision and 89.50% recall, as shown in fig. 5.11. However, the false negative rate is as high as 10.5%, which implies that the classifier is not good at detecting users intention to stop as detecting user start.

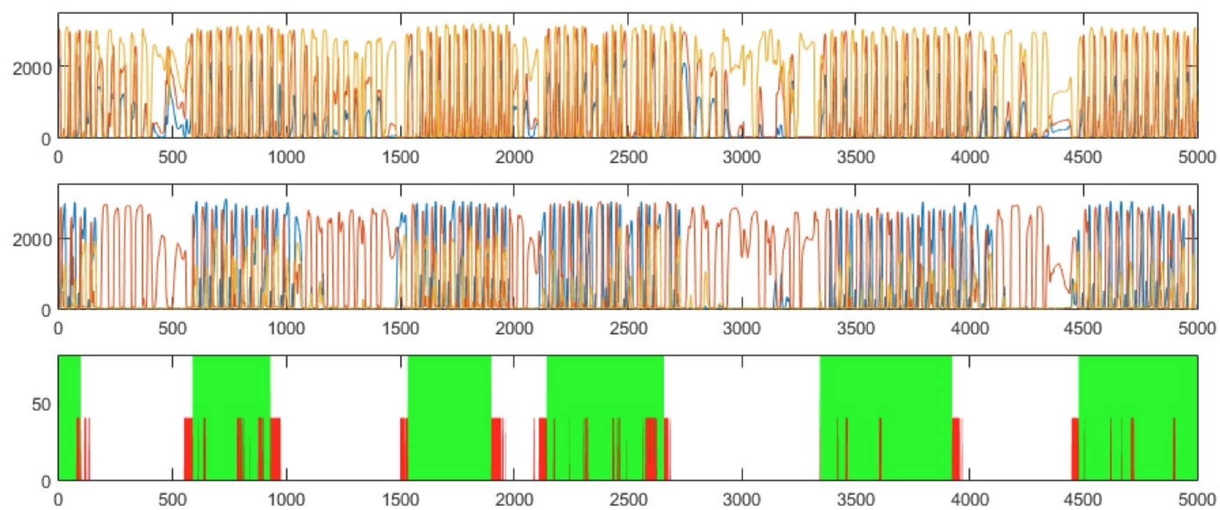

Figure 5.10: Test result of SVM

When combining SVM with Adaboost, the test error stagnates at around 9% over 30 iterations while the training error shows a marginal improvement as it drops from 0.3% to 0.16%. This is likely due to limitation of window slicing method and SVM classifier incapable of learning the complex decision boundary. Overall, SVM has demonstrated an excellent performance for real-time gait classification.

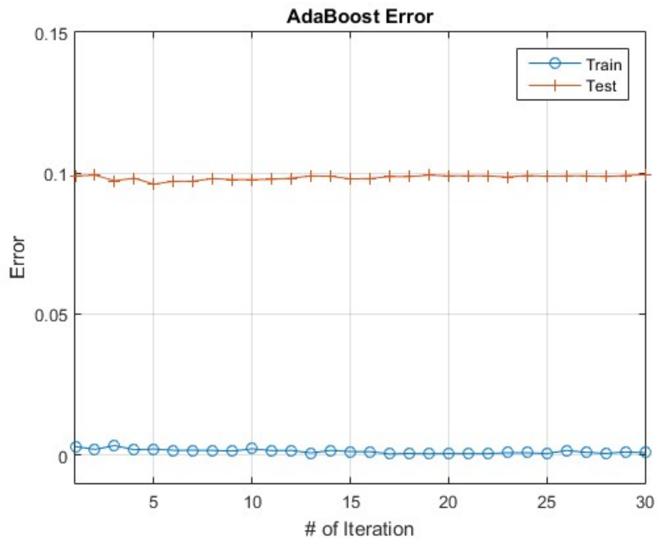

Figure 5.11: Adaboost error plot

Chapter 6: Motor control

It is a challenging task to fit motor, control electronics and transmission system just under the area of a shoe plus significantly high torque and efficiency requirements. Despite its low cost and simple control, a traditional DC motor has insufficient power density and efficiency due to increasing brush friction at higher speed. In order to address the above issues while keeping the cost low, a hobbyist grade brushless DC (BLDC) motor with a custom control electronics is used in this project.

Both heel strike and push off phases exert significant disturbance to the BLDC motor which is controlled at constant speed, causing a significant speed reduction, which is undesirable. In addition to the trapezoidal BLDC control, this thesis modifies and implements a disturbance-observer-based control method that was previously used on large permanent-magnet synchronous motors.

6.1 Related work

In order to reject disturbance for motor control, a feed-forward compensation part could be introduced Back and Shim [2], Wu [29]. However, since usually it is impossible to measure the disturbance directly, it has to be estimated and varied methods have been proposed, such as disturbance-observer-based (DOB) control method (Chen et al. [7], Ko and Han [14]), and extended state observer (ESO) method (Han [10], Li and Liu [16]). For instance, Chen et al. [7] developed a nonlinear disturbance observer for two link robotic manipulators, Li and Liu [16] used ESO to estimate both states and lumped disturbances simultaneously, and Han [10] proposed an active disturbance rejection control by employing a feed-forward compensation based on ESO.

6.2 Algorithm

Although the low-level computation control using zero-crossing method has shown a satisfactory result, the top level speed regulation via PI control is still susceptible to varying load. So the goal of new motor controller design is to improve its disturbance rejection performance while maintaining a relatively low control input. We decided to use a combination of feed-forward and feedback control to achieve this goal.

6.2.1 BLDC parameter estimation

In order to build a feed-forward controller, we first estimate motor parameters. We adopt DC motor parameter identification based on dynamic parametrization of the motor speed response under a constant voltage input. It is more practical and cost effective since it requires only a sensorless speed controller which samples motor speed and supplying voltage. The curve fitting performed by minimizing the sum of the square error via gradient descent.

Consider the following state space representation of DC motor,

$$\begin{aligned} \frac{d}{dt}\begin{bmatrix} \dot{\theta} \\ \dot{i} \end{bmatrix} &= \begin{bmatrix} -\frac{b}{J} & \frac{K_b}{J} \\ -\frac{K_t}{L} & -\frac{R}{L} \end{bmatrix} \begin{bmatrix} \dot{\theta} \\ i \end{bmatrix} + \begin{bmatrix} 0 \\ \frac{1}{L} \end{bmatrix} V \\ y &= \begin{bmatrix} 1 & 0 \end{bmatrix} \begin{bmatrix} \dot{\theta} \\ i \end{bmatrix} \end{aligned} \tag{6.1}$$

Where L is the inductivity, i is the winding current, R is the terminal resistance, k_b is the back-EMF constant, w is the motor speed, J is the moment of inertia, V is the motor terminal voltage, b is the rotational damping coefficient, k_t is the torque constant, which is an inverse of k_b.

Given terminal voltage and target output, we can derive a gradient descent algorithm (algorithm 1) to minimize the sum of the square error between target output and simulated output, $\vec{w} \leftarrow \arg\min_w \sum_l (y^l - f(v^l))^2$, where the threshold is set to be 0.001 between the last and current iteration error result or 100 iterations.

Algorithm 1 Gradient Descent for updating motor parameters

1: l = l^{th} sampled voltage and motor speed
2: $\vec{w} = [l, R, k_b, J, b]$
3: **while** Not Satisfied **do**
4: $\quad \nabla E = [\frac{\partial E}{\partial L}, \frac{\partial E}{\partial R}, \frac{\partial k_b}{\partial R}, \frac{\partial J}{\partial R}, \frac{\partial b}{\partial R}]$
5: $\quad \vec{w} = \vec{w} - \eta \nabla E[\vec{w}]$
6: **end while**

The combined scheme adds two feed-forward terms in addition to the initial PI controller as shown in fig. 6.1 . The goal is to reduce the overshoot induced by feedback term and improve disturbance rejection performance.

The inverse BLDC dynamics is approximated as a DC gain which is the ratio of the steady state velocity of the BLDC motor to its constant voltage input.

$$DCG = \lim_{s \to 0} G(s) \tag{6.2}$$

6.2.2 Disturbance rejection

For motor speed regulation applications, especially at the steady state, the periodical disturbance torque that is caused by foot push-off can cause the speed ripples. If the disturbance can be quantified, a voltage can be applied to the motor to counteract the disturbance torque and minimizes

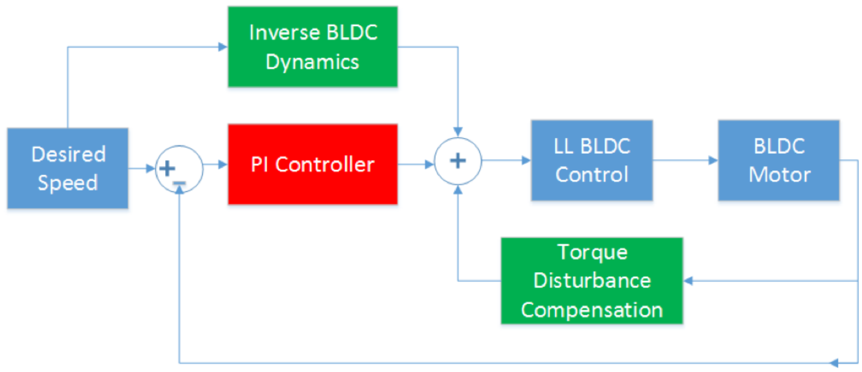

Figure 6.1: Combined feedforward and feedback control scheme

the speed ripples as mentioned in Wu [29]. To accomplish this, an on-line estimation of the disturbance and a feed-forward control law that generates the counteracting voltage is constructed. The speed response in the Laplace domain is:

$$w = \frac{\frac{1}{k_b}}{t_e t_m s^2 + t_m s + 1}(V + V_{ff}) - \frac{\frac{t_m t_e}{J} s + \frac{t_m}{J}}{t_e t_m s^2 + t_m s + 1} T_d \tag{6.3}$$

Where $t_e = \frac{L}{R}$ is the electrical time constant and $t_e = \frac{RJ}{k_b k_t}$ is the mechanical time constant. Here we will choose V_{ff} to cancel the effect of T_d on w which means:

$$V_{ff}(s) = (\frac{L}{k_t} s + \frac{R}{k_t}) T_d(s) \tag{6.4}$$

This is then implemented on the hardware in discrete form:

$$V_{ff}(k) = (\frac{L}{k_t \Delta t} + \frac{R}{k_t}) T_d(k) - \frac{L}{k_t \Delta t} T_d(k-1) \tag{6.5}$$

Substitute T_d with $k_t * i$ (we ignore the inertia term as the moment of inertia is very small and the acceleration signal is extremely noisy and unusable), thus, we can use the following equation to compute V_{ff}:

$$V_{ff}(k) = (\frac{L}{\Delta t} + R) i(k) - \frac{L}{\Delta t} i(k-1) \tag{6.6}$$

6.3 Results

The top plot of Figure 6.2 shows the measured output voltage vs estimated output after gradient descent while the bottom plot shows the input voltage based on the commanded duty cycle. Several initial conditions have been experimented and the figure represents the smallest sum of the squared error.

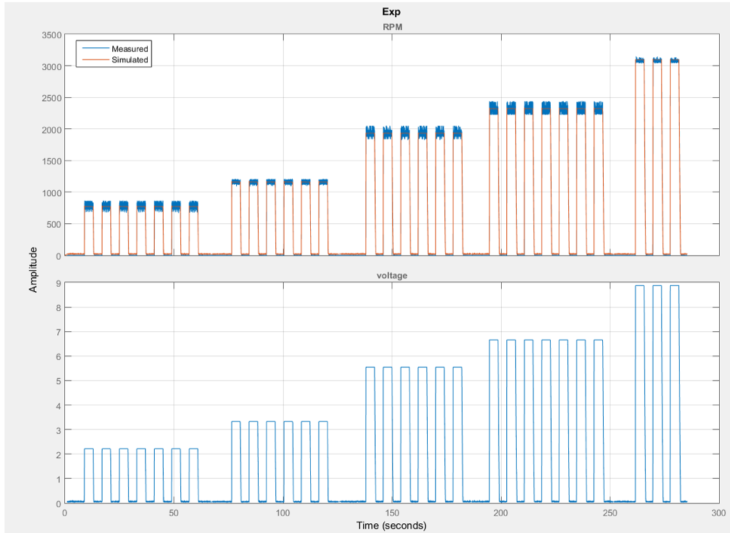

Figure 6.2: The top plot shows the measured output voltage vs estimated output after gradient descent while the bottom plot shows the input voltage based on the commanded duty cycle

Next we compare the controllers performance by commanding the motor to stabilize 600 rpm and observing measured current which is proportional to the disturbance torque that motor experienced. In 6.3 and 6.4, when both motors are experienced with similar disturbance torque, the conventional PI controller exhibits much larger speed ripples with near 100 percent max overshoot, while the combined control scheme maintains a much more constant speed with only ± 16 percent oscillation around the steady state velocity.

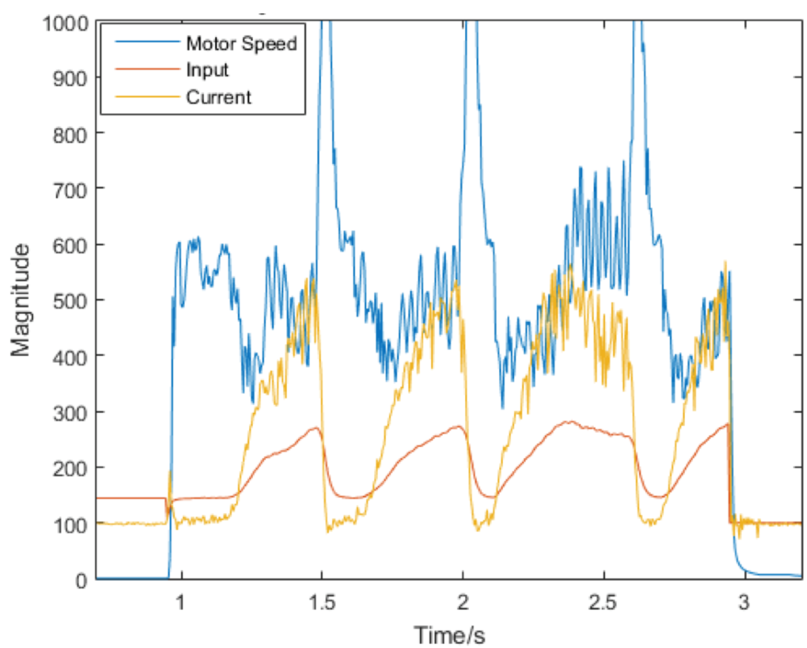

Figure 6.3: Disturbance rejection without feed-forward control

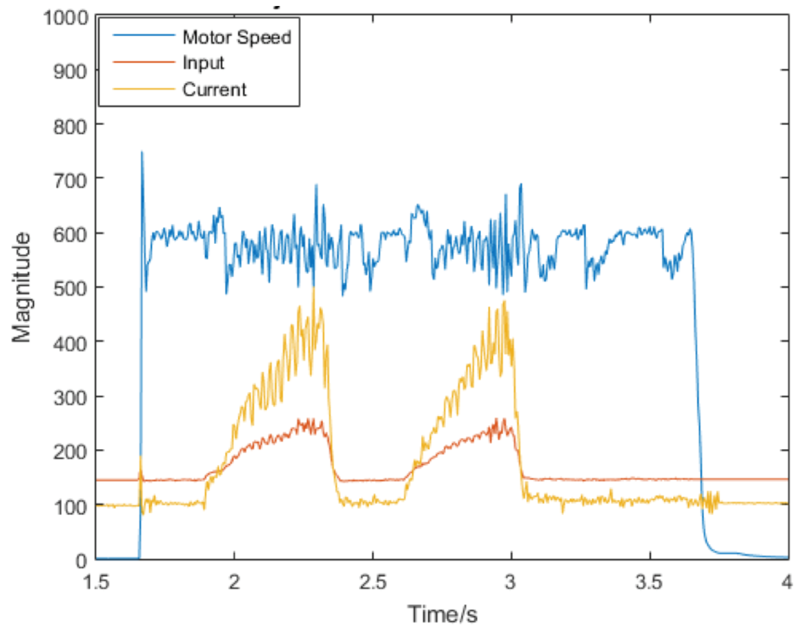

Figure 6.4: Disturbance rejection with feed-forward control

In order to compare the controllers performance on actual prototype, the combined control scheme was implemented on the actual shoes. A series of body swinging motions were performed to introduce a cyclic disturbance load, as shown in figure 6.5 (note that current is scaled up in the figure to be visualized with speed ripples all together). The combined control scheme is able to maintain a much more stable speed with significantly smaller speed ripples and overshoots, when compared with the conventional PI controller.

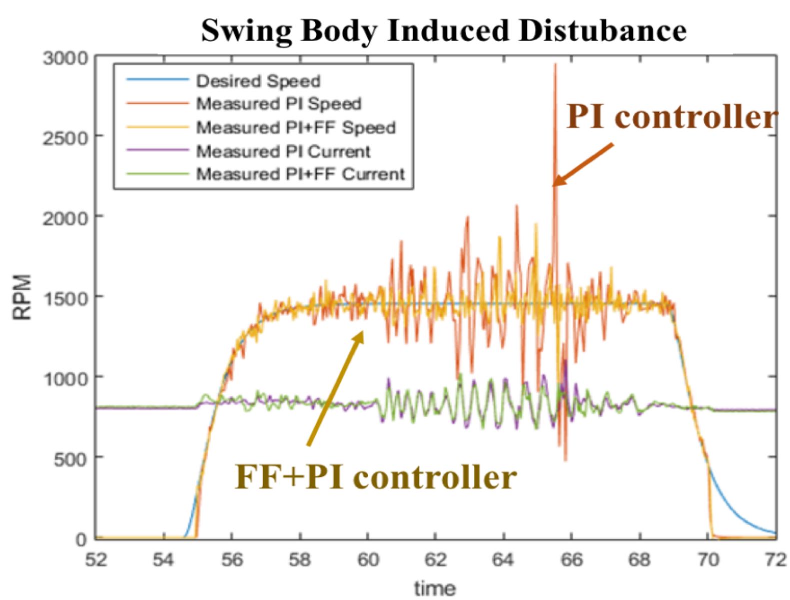

Figure 6.5: Swing body induced disturbance

Based on the BLDC motor parameter estimation, we have computed disturbance torque from measured current and derived control laws to reject the disturbance. Experimental results in both bench and prototype tests show that the combined scheme has a superior disturbance rejection, stability and system responsiveness than the conventional PI controller.

Chapter 7: Conclusion

In this paper, we have identified the first-last mile challenge as the major barrier to the use of public transport and addressed this challenge by designing a control system of a personal mobility device that enables average pedestrians to double their walking speed. We focused on identifying the target customers and their pain point when commuting, breaking down the user pain points into product requirements. Most importantly, by recognizing the technical challenge of bipedal walking control, we have identified gait predication as the key research question and attempted two approaches: VMC based gait prediction and machine learning based gait classification. The latter approach was selected for its performance and ability to generalize in various gaits. Due to the challenging space constraints and high power throughput requirements, a disturbance-observer-based controller is used to control a BLDC motor as a single power system for each bionic shoe. In the future, I plan to develop more rigorous customer research to further capture the user experience and improve upon the technology that addresses those pain points.

Bibliography

[1] Murad Alaqtash, Thompson Sarkodie-Gyan, Huiying Yu, Olac Fuentes, Richard Brower, and Amr Abdelgawad. Automatic classification of pathological gait patterns using ground reaction forces and machine learning algorithms. In *Engineering in Medicine and Biology Society, EMBC, 2011 Annual International Conference of the IEEE*, pages 453–457. IEEE, 2011. 5.3.1

[2] Juhoon Back and Hyungbo Shim. Adding robustness to nominal output-feedback controllers for uncertain nonlinear systems: A nonlinear version of disturbance observer. *Automatica*, 44(10):2528–2537, 2008. 6.1

[3] Carl Bialik. New yorkers will pay 56 a month to trim a minute off their commute. https://fivethirtyeight.com/features/new-yorkers-will-pay-56-a-month-to-trim-a-minute-off-their-commute/, August 2016. 1

[4] Raymond C Browning and Rodger Kram. Effects of obesity on the biomechanics of walking at different speeds. *Medicine and Science in Sports and Exercise*, 39(9):1632, 2007. 5.2.3

[5] Peter R Cavanagh and Mario A Lafortune. Ground reaction forces in distance running. *Journal of biomechanics*, 13(5):397–406, 1980. 5.3.1

[6] Paul Chavand. Wheeled shoes or undersoles enabling fast walking, May 12 2015. US Patent 9,027,690. 4.1

[7] Wen-Hua Chen, Donald J Ballance, Peter J Gawthrop, Jeremy J Gribble, and John O Reilly. A nonlinear disturbance observer for two link robotic manipulators. In *Decision and Control, 1999. Proceedings of the 38th IEEE Conference on*, volume 4, pages 3410–3415. IEEE, 1999. 6.1

[8] Sara J Cuccurullo. *Physical medicine and rehabilitation board review*. Demos Medical Publishing, 2014. 2

[9] Ross Cutler and Larry S Davis. Robust real-time periodic motion detection, analysis, and applications. *Pattern Analysis and Machine Intelligence, IEEE Transactions on*, 22(8): 781–796, 2000. 5.3.1

[10] Jingqing Han. From pid to active disturbance rejection control. *Industrial Electronics, IEEE transactions on*, 56(3):900–906, 2009. 6.1

[11] Jianjuen J Hu, Jerry E Pratt, Chee-Meng Chew, Hugh M Herr, and Gill A Pratt. Virtual model based adaptive dynamic control of a biped walking robot. *International Journal on*

Artificial Intelligence Tools, 8(03):337–348, 1999. 5.2, 4

[12] Sandra R Hundza, William R Hook, Christopher R Harris, Sunny V Mahajan, Paul A Leslie, Carl A Spani, Leonhard G Spalteholz, Benjamin J Birch, Drew T Commandeur, and Nigel J Livingston. Accurate and reliable gait cycle detection in parkinson's disease. *Neural Systems and Rehabilitation Engineering, IEEE Transactions on*, 22(1):127–137, 2014. 5.3.1

[13] Shuuji Kajita, Fumio Kanehiro, Kenji Kaneko, Kiyoshi Fujiwara, Kensuke Harada, Kazuhito Yokoi, and Hirohisa Hirukawa. Biped walking pattern generation by using preview control of zero-moment point. In *Robotics and Automation, 2003. Proceedings. ICRA'03. IEEE International Conference on*, volume 2, pages 1620–1626. IEEE, 2003. 5.3.1

[14] Jong-Sun Ko and Byung-Moon Han. Precision position control of pmsm using neural network disturbance observer on forced nominal plant. In *Mechatronics, 2006 IEEE International Conference on*, pages 316–320. IEEE, 2006. 6.1

[15] Lily Lee and W Eric L Grimson. Gait analysis for recognition and classification. In *Automatic Face and Gesture Recognition, 2002. Proceedings. Fifth IEEE International Conference on*, pages 148–155. IEEE, 2002. 5.3.1

[16] Shihua Li and Zhigang Liu. Adaptive speed control for permanent-magnet synchronous motor system with variations of load inertia. *Industrial Electronics, IEEE Transactions on*, 56(8):3050–3059, 2009. 6.1

[17] Brian McKenzie. Modes less traveledbicycling and walking to work in the united states: 2008–2012. *US Census Bureau, New York*, 2014. 1

[18] Serafeim P Moustakidis, John B Theocharis, and Giannis Giakas. Subject recognition based on ground reaction force measurements of gait signals. *Systems, Man, and Cybernetics, Part B: Cybernetics, IEEE Transactions on*, 38(6):1476–1485, 2008. 5.3.1

[19] AMS Muniz and J Nadal. Application of principal component analysis in vertical ground reaction force to discriminate normal and abnormal gait. *Gait & posture*, 29(1):31–35, 2009. 5.3.1

[20] AMS Muniz, H Liu, KE Lyons, R Pahwa, W Liu, FF Nobre, and J Nadal. Comparison among probabilistic neural network, support vector machine and logistic regression for evaluating the effect of subthalamic stimulation in parkinson disease on ground reaction force during gait. *Journal of Biomechanics*, 43(4):720–726, 2010. 5.3.1

[21] Marko B Popovic, Ambarish Goswami, and Hugh Herr. Ground reference points in legged locomotion: Definitions, biological trajectories and control implications. *The International Journal of Robotics Research*, 24(12):1013–1032, 2005. 5.3.1

[22] Jerry Pratt, Chee-Meng Chew, Ann Torres, Peter Dilworth, and Gill Pratt. Virtual model control: An intuitive approach for bipedal locomotion. *The International Journal of Robotics Research*, 20(2):129–143, 2001. 5.1

[23] Eric Ries. *The lean startup: How today's entrepreneurs use continuous innovation to create radically successful businesses*. Crown Business, 2011. 2

[24] Sandra Shultz, Peggy Houglum, and David Perrin. *Examination of Musculoskeletal Injuries*

with Web Resource. Human Kinetics, 2015. 5.1

[25] Margaret M Skelly and Howard Jay Chizeck. Real-time gait event detection for paraplegic fes walking. *Neural Systems and Rehabilitation Engineering, IEEE Transactions on*, 9(1): 59–68, 2001. 5.3.1

[26] Peter Treadway, Janelle Wang Treadway, and Hang Zheng. Wearable personal transportation system, June 10 2015. US Patent App. 14/736,064. 4.1

[27] Miomir Vukobratović and Branislav Borovac. Zero-moment pointthirty five years of its life. *International Journal of Humanoid Robotics*, 1(01):157–173, 2004. 5.3.1

[28] David A Winter. Human balance and posture control during standing and walking. *Gait & posture*, 3(4):193–214, 1995. 5.1, 3

[29] Wei Wu. Disturbance compensation for dc motor mechanism low speed regulation: A feedforward and feedback implementation. In *Decision and Control and European Control Conference (CDC-ECC), 2011 50th IEEE Conference on*, pages 1614–1619. IEEE, 2011. 6.1, 6.2.2

[30] Bai-ling Zhang, Yanchun Zhang, and Rezaul K Begg. Gait classification in children with cerebral palsy by bayesian approach. *Pattern Recognition*, 42(4):581–586, 2009. 5.3.1